Supporting information

Interlayer interaction force-tuned molecular magnets in Co^{II}-tetrazolate-carboxylate system from canted antiferromagnet to field-induced metamagnet

Bo Ding, Zhong-Yi Liu, Xin-Jing Gong, Hui-Min Tang, Xiu-Guang Wang, Zheng-Yu Liu, Hui-Ming Dong,

Jing Liu and En-Cui Yang

Materials and general methods. All the initial chemicals were commercially purchased (Hmtz, H$_2$pyzdc, and H$_3$btc were from Acros and other analytical-grade reagents were from Tianjin chemical reagent factory) and used as received without further purification. Elemental analyses for C, H, and N were carried out with a CE-440 (Leeman-Labs) analyzer. Fourier transform (FT) IR spectra (KBr pellets) were taken on an Avatar-370 (Nicolet) spectrometer in the range 4000–400 cm^{-1}. Thermogravimetric analysis (TGA) experiment was performed on a Shimadzu simultaneous DTG-60A compositional analysis instrument from room temperature to 800 ^{o}C in a N$_2$ atmosphere at a heating rate of 5 ^{o}C min^{-1}. Powder X-ray diffraction (PXRD) patterns were obtained from a Bruker D8 ADVANCE diffractometer at 40 kV and 40 mA for Cu Kα radiation (λ = 1.5406 Å), with a scan speed of 0.1 sec/step and a step size of 0.01 ^{o} in 2θ. The simulated PXRD pattern was calculated using single-crystal X-ray diffraction data and processed by the free Mercury v1.4 program provided by the Cambridge Crystallographic Data Center. Magnetic susceptibilities were acquired on a Quantum Design (SQUID) magnetometer MPMS-XL-7 with crystalline samples, in which the phase purity of the samples was determined by PXRD experiments. The data were corrected for TIP and the diamagnetic corrections were calculated using Pascal's constants. An experimental correction for the sample holder was also applied.

Table S1. Selected bond lengths (Å) and angles (deg) for **1** ^{a}

Co(1)–O(2)	2.028(2)	Co(2)–O(1)$^{\#3}$	2.027(2)
Co(1)–O(4)$^{\#1}$	2.048(2)	Co(2)–O(5)$^{\#1}$	2.091(2)
Co(1)–N(3)$^{\#2}$	2.087(3)	Co(2)–O(4)	2.055(2)
Co(1)–O(7)	2.094(2)	Co(2)–N(1)	2.145(3)
Co(1)–O(5)$^{\#1}$	2.125(2)	Co(2)–N(4)$^{\#4}$	2.177(3)
Co(1)–N(2)	2.131(3)		
O(5)$^{\#1}$–Co(1)–N(2)	81.97(10)	O(2)–Co(1)–O(4)$^{\#1}$	91.84(9)
O(7)–Co(1)–N(2)	85.47(10)	O(2)–Co(1)–N(3)$^{\#2}$	88.53(10)
O(7)–Co(1)–O(5)$^{\#1}$	98.57(9)	O(4)$^{\#1}$–Co(1)–N(3)$^{\#2}$	87.70(10)
O(4)$^{\#1}$–Co(1)–O(5)$^{\#1}$	84.43(9)	O(4)$^{\#1}$–Co(1)–O(7)	96.22(9)
O(2)–Co(1)–N(2)	87.74(10)	N(3)$^{\#2}$–Co(1)–O(7)	87.34(10)
O(1)$^{\#3}$–Co(2)–N(4)$^{\#4}$	89.90(10)	O(2)–Co(1)–O(5)$^{\#1}$	86.62(9)
O(4)–Co(2)–N(1)	93.69(10)	N(3)$^{\#2}$–Co(1)–N(2)	105.88(11)
O(4)–Co(2)–O(5)$^{\#1}$	107.21(9)	O(4)–Co(2)–N(4)$^{\#4}$	85.16(10)
O(1)$^{\#3}$–Co(2)–N(1)	95.57(10)	O(5)$^{\#1}$–Co(2)–N(4)$^{\#4}$	91.47(10)
O(5)$^{\#1}$–Co(2)–N(1)	83.75(10)	O(1)$^{\#3}$–Co(2)–O(4)	103.08(9)
O(1)$^{\#3}$–Co(2)–O(5)$^{\#1}$	149.68(10)		

^{a} Symmetry codes: $^{\#1}$ 1/2 − x, y − 1/2, 1/2 − z; $^{\#2}$ 1/2 − x, 1/2 − y, −z; $^{\#3}$ 1/2 − x, y + 1/2, 1/2 − z; $^{\#4}$ x, 1 − y, z + 1/2.
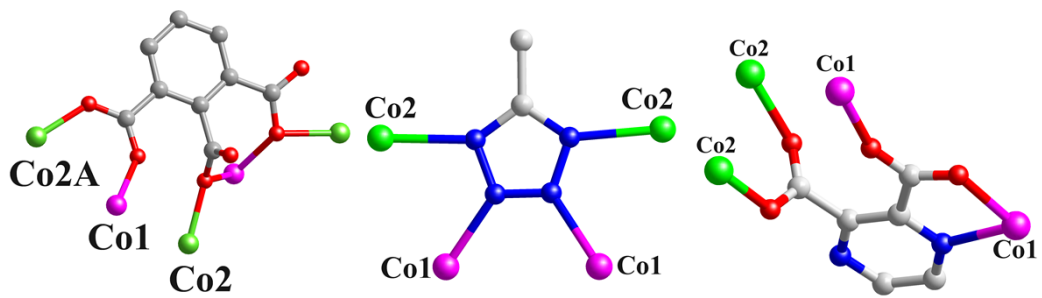
Fig. S1. Binding mode of btc^{3-}, mtz$^-$, and pyzdc^{2-} ligands in **1** and **2**.

Table S2. Hydrogen-bonding parameters (Å, deg) for **1** [a]

D – H···A	d (D–H)	d (H···A)	d (D···A)	∠DHA
O7–H7B···O8[#1]	0.884	1.936	2.752	152.79

[a] Symmetry codes: [#1] $1/2 - x, y - 1/2, -z + 1/2$.

Table S3. Selected bond lengths (Å) and angles (deg) for **2** [a]

Co(1)–N(2)	2.198(3)	Co(1)–N(2)$^{\#2}$	2.198(3)
Co(1)–O(4)	2.107(3)	Co(1)–N(3)	2.171(3)
Co(1)–O(2)$^{\#1}$	2.021(3)	Co(1)–O(1)	2.063(3)
Co(2)–N(1)	2.100(2)	Co(2)–O(3)$^{\#4}$	2.102(2)
Co(2)–O(4)	2.0776(17)	O(2)$^{\#1}$–Co(1)–O(4)	92.36(11)
O(1)–Co(1)–O(4)	91.00(11)	O(2)$^{\#1}$–Co(1)–N(3)	100.05(13)
O(1)–Co(1)–N(3)	76.59(12)	N(3)–Co(1)–N(2)	93.63(7)
O(2)$^{\#1}$–Co(1)–N(2)	89.32(8)	O(1)–Co(1)–N(2)	90.89(8)
O(4)–Co(1)–N(2)	86.46(7)	O(4)–Co(2)–O(3)$^{\#4}$	88.29(10)
N(1)–Co(2)–O(3)$^{\#1}$	89.97(9)	O(4)–Co(2)–N(1)	85.28(9)

[a] Symmetry codes: $^{\#1}$ $x − 1/2, y, 3/2 − z$;$^{\#2}$ $x, 1/2 − y, z$; $^{\#3}$ $− x, −y, 2 − z$; $^{\#4}$ $1/2 − x, − y, z + 1/2$.
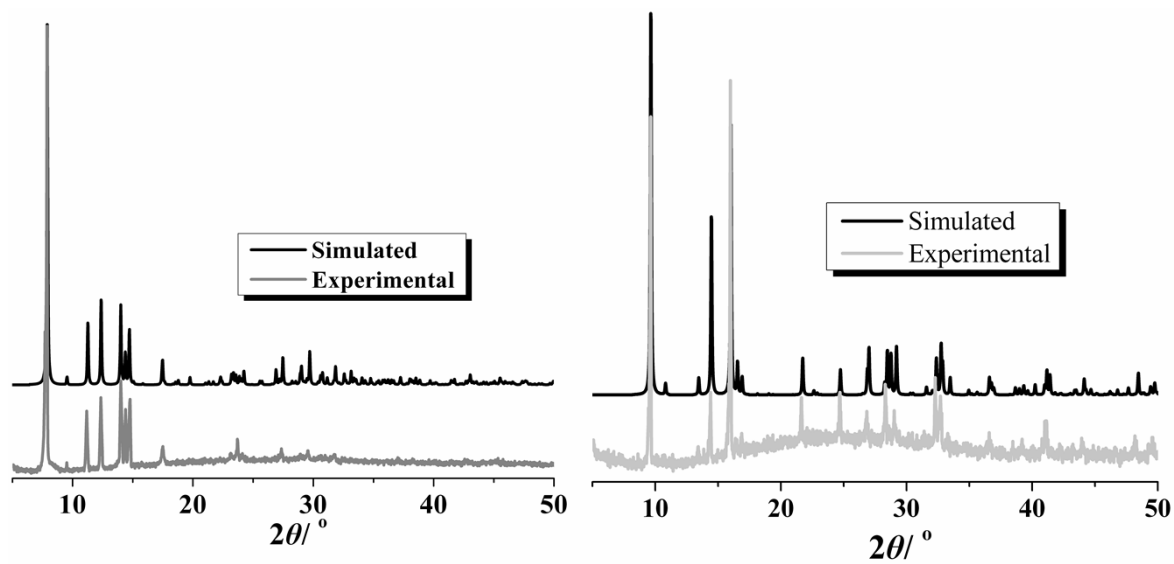
Fig. S2. XPRD patterns for **1** and **2**.
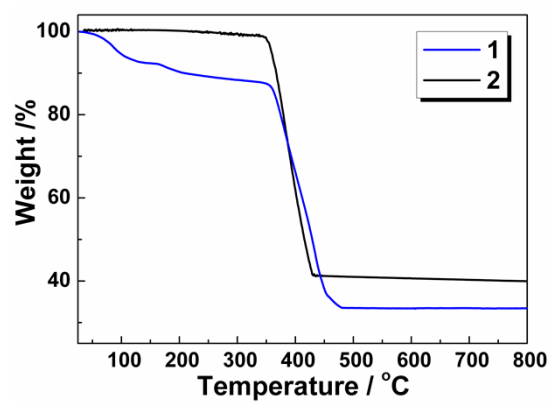
Fig. S3. TG curves for **1** and **2**.
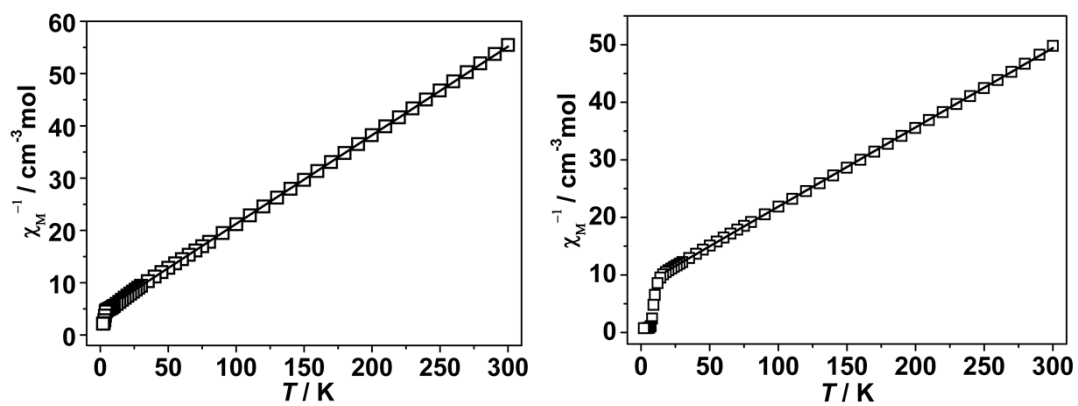
Fig. S4. Plots of χ_M^{-1} *vs.* T for **1** (left) and **2** (right) in an applied field of 2.0 kOe (The straight line represents the best fit to the Curie-Weiss law).
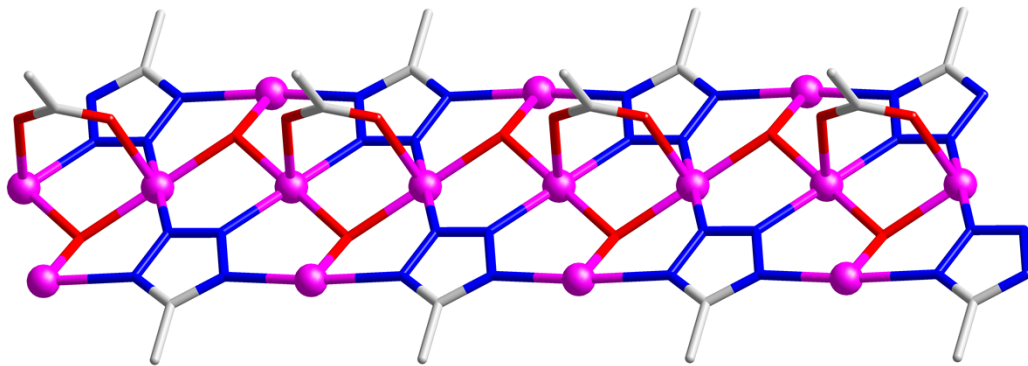
Fig. S5. Magnetic bridges within the corner-sharing Δ-ribbon of **2**.